

Effects of higher modes on vertical distribution of isolated structures under near field earthquakes

F. Khoshnoudian^{1,*}, O. Nozadi²

Received: June 2012, Revised: November 2012, Accepted: January 2013

Abstract

It has been pointed out the static lateral response procedure for a base-isolated structure proposed in International Building Code (IBC) somewhat overestimates the seismic story force. That is why in the current paper, vertical distribution of base shear over the height of isolated structures considering higher mode effects under near field earthquakes is investigated. Nonlinear behavior of isolation systems cause variation of frequencies transmitted to the superstructure and consequently higher modes effects should be considered. In this study base shear distribution obtained from nonlinear dynamic analysis is compared with that achieved from IBC for assessment of the international building code. This investigation has been conducted in two parts, in order to have an appropriate base shear distribution formula for isolated structures under near field earthquakes. In the first part using three first mode shapes of isolated structure and introducing coefficient corresponding to each mode, extracted from nonlinear dynamic analysis under near field earthquakes, a new formula has been derived. In the second part, the mode shape coefficients have been obtained theoretically and consequently a new base shear distribution over the height of isolated structures including the isolation system properties under near field ground motions was proposed.

Keywords: Base-isolated structures, Base shear distribution, Near field earthquake, Higher modes effects.

1. Introduction

Seismic design of structures is based on increasing the resistance capacity of the structure against earthquakes; however it causes higher accelerations at the floors or increasing of drift in flexible structures. This means during the strong earthquake motions although the structure does not collapse, nonstructural components are damaged significantly. It is not acceptable for buildings equipped with more valuable contents such as telecommunication center or hospitals which need to be operated immediately after the earthquakes [1].

In order to solve this problem, isolation systems are employed in the structures. Using the isolators a shift in the period of system is noticed. By increasing this period acceleration exerted on superstructure due to earthquake is reduced and eventually seismic forces on the superstructure are decreased [2]. Also this prevents the period of system to fall within the range of earthquake dominant frequency,

resulting in the prevention of resonance phenomenon [3].

It is observed that the isolation systems have nonlinear behavior. This characteristic results in major portion of the earthquake energy to dissipate by isolation system. Therefore the structural deformations remain within the elastic range [2]. According to UBC-91[4], the vertical distribution of lateral forces is based on this assumption that motion of the superstructure is similar to a rigid body motion, thus the acceleration in the stories is uniform. Based on this suggestion distribution of the lateral forces is proportional to the mass of story:

$$F_x = \frac{V_s w_x}{\sum_{i=1}^n w_i} \quad (1)$$

w_x and w_i : the weight of stories at x and i levels

F_x : the force at the x level

Since effects of the higher modes are not considered, it causes non-conservative results. According to UBC-97[5], and IBC [6], base shear distribution (V_s) over the height of structure can be obtained by following equation:

$$F_x = \frac{V_s w_x h_x}{\sum_{i=1}^n w_i h_i} \quad (2)$$

* Corresponding Author: Khoshnud@aut.ac.ir
1 Associate Professor, Faculty of Civil Engineering, Amirkabir University of Technology, Tehran, Iran.
2 MSc graduated, Faculty of Civil Engineering, Amirkabir University of Technology, Tehran, Iran.

Where h_x and h_i represent height of stories at x and i levels. This triangular shear distribution for isolated structure is similar to fixed base structures. The previous investigations demonstrate that the triangular distribution is always a conservative estimation comparing to the exact distribution obtained from nonlinear dynamic analysis. In addition the base shear distribution can be indicated as following according to Eurocode [7]:

$$F_x = m_x S_e (T_{eff}) S_{eff} \quad (3)$$

F_x : xth story shear force
 m_x : mass of the xth story
 T_{eff} and S_{eff} : effective period and damping of the isolation system respectively
 S_e : spectral acceleration

Vertical distribution of lateral forces on structures except for the non-reinforced masonry buildings can be obtained as [8]:

$$F_x = C_{vx} V \quad (4)$$

$$C_{vx} = \frac{w_x h_x^k}{\sum_{i=1}^n w_i h_i^k} \quad (5)$$

C_{vx} is vertical distribution coefficient, $k=2.0$ for $T \geq 2.5$ sec, $k=1.0$ for $T \leq 0.5$ sec and for $0.5 \text{ sec} < T < 2.5 \text{ sec}$ k values are obtained by linear interpolation.

Lee and Kim studied vertical distribution of base shear for base-isolated structures [9]. They proposed formula based on the dynamic of a two-mass linear system as follows:

$$F_x = \frac{w_x (1 + \frac{\varepsilon h_x}{\mu h_n})}{\sum w_i (1 + \frac{\varepsilon h_i}{\mu h_n})} V_s \quad (6)$$

Where $\varepsilon = (\omega_b^2 / \omega_s^2)$ and also ω_b and ω_s are fixed-base and isolation system frequencies, respectively. μ is the effective height coefficient and h_n is the height of the structure. Donatello, Cardone and Mauro Dolce proposed a formula for vertical distribution of base shear [10]. They Considered nonlinearity, period of isolation system and period of superstructure and proposed equations for first three mode shapes.

$$\Delta_{1i} = \phi_{1i} \quad (7)$$

$$\Delta_{2i} = \phi_{1i} + a_2 \phi_{2i} \quad (8)$$

$$\Delta_{3i} = \phi_{1i} + a_2 \phi_{2i} + a_3 \phi_{3i} \quad (9)$$

Where Δ_{1i} , Δ_{2i} and Δ_{3i} are profile of displacement, ϕ_{1i} , ϕ_{2i} and ϕ_{3i} are first three mode shapes, a_2 and a_3 are coefficients related to characteristics of isolation system and superstructure.

Khoshnoudian and Esrafilii proposed a formula for base shear distribution as follows [11]:

$$F_x = \frac{V_s}{n+1} ([A] + \eta[B] + \rho[C]) \quad (10)$$

Where $[A]$, $[B]$ and $[C]$ are first three simplified mode shapes of isolated structures. η and ρ are coefficients that obtained from using nonlinear dynamic analysis and n is number of story. In addition Khoshnoudian and Mehrparvar proposed a new formula for vertical distribution of base shear over the height of isolated structures as follows [12]:

$$F_x = \mu \frac{w_x}{\sum_{i=1}^n w_i} V_s + (1 - \mu) \frac{w_x h_x}{\sum_{i=1}^n w_i h_i} V_s \quad (11)$$

Where μ is a coefficient that obtained from comparison of nonlinear dynamic analysis with proposed formula.

In the previous investigations, simplified formulas were proposed without including isolation properties for equivalent lateral response procedure and the earthquake ground motions were assumed far field earthquakes. That is why in the current paper, the objective is to propose a new formula for vertical distribution of base shear for equivalent lateral response procedure considering near field earthquakes and in addition attempt is made to include the isolation system properties in the proposed formula.

2. Modeling of super-structure and isolation system

In this investigation full 3-D models of isolated structures were analyzed by ETABS computer program (based on 3D-basis program) (ETABS, 1999). The super-structures and isolators were modeled using linear and nonlinear behaviors respectively. Nllink elements in ETABS were used for modeling elastomeric nonlinear isolators. The element has coupled plasticity properties for two shear deformations and linear effective properties for the remaining four deformations. The plasticity model is based on the hysteretic behavior proposed by Wen [19], and Park et al [14], and recommended for base isolation analysis by Nagarajaiha et al [18]. The building models under consideration have symmetric plan (Fig.1) and distribution of mass and stiffness is uniform through the height. The structures consist of 2, 4 and 6 stories assuming story height of 3.5m. Ordinary steel moment frames are employed in this investigation. Steel structures have been designed according to American Institute of Steel Construction

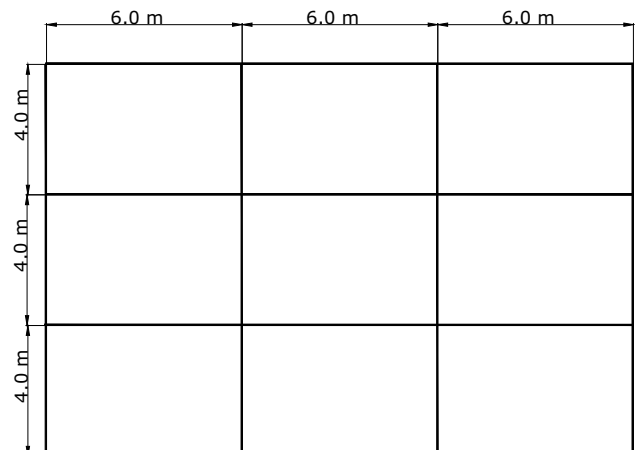


Fig. 1 Plan of structure

(AISC-ASD) [13]. Cross sections of beams and columns are shown in table 1. In addition, the structural properties (periods and effective modal mass of the first 3 modes) are presented in table 2.

Six types of isolation systems have been used in this study. The isolators are supposed elastomeric and are modeled by bi-linear hysteresis behavior having plastic behavior for two shear deformations. Effective linear stiffness for other deformations is assumed constant. Plasticity model is on the basis of hysteretic behavior proposed by Wen et al. [14]. Isolation system parameters involve initial stiffness (K_1), secondary stiffness (K_2), effective stiffness (K_{eff}), intersection of hysteresis cycle and vertical axis (Q) and period (T) (Fig. 2). Table 3 shows the properties of selected isolation systems, where W stands for the structure effective weight. Considering Fig.2 the following equations can be derived:

$$D_y = \frac{Q}{K_1 - K_2} \quad (12)$$

$$K_{eff} = K_2 + \frac{Q}{D} \quad (13)$$

Table 1 Cross sections of beams and columns

No of stories	Column section(cm)	Beam section (X dir.)	Beam section (Y dir.)
2	BOX 20×20 ×1.6	IPE330	IPE200
4	BOX 24×24 ×1.6	IPE360	IPE220
6	BOX 30×30 ×1.6	IPE360	IPE240

Table 2 Structural properties (periods and effective modal mass of the first 3 modes)

No. of stories	First mode		Second mode		Third mode		
	Period	Modal mass	Period	Modal mass	Period	Modal mass	
2	2(s)	2.46	99.9801	0.72	0.0193	0.26	0.0006
	2.5(s)	2.95	99.9884	0.72	0.0113	0.26	0.0003
	3(s)	3.46	99.9945	0.72	0.0054	0.26	0.0001
4	2(s)	2.26	99.8151	0.42	0.1771	0.19	0.0069
	2.5(s)	2.73	99.9218	0.42	0.0751	0.19	0.0028
	3(s)	3.35	99.9624	0.42	0.0361	0.19	0.0013
6	2(s)	2.14	99.6251	0.44	0.3527	0.22	0.0195
	2.5(s)	2.67	99.8377	0.45	0.1532	0.22	0.008
	3(s)	3.22	99.921	0.45	0.0748	0.22	0.0038

Table 3 Properties of isolation systems

Isolation system type	T(s)	Effective Damping(%)	Q	K_1	$\frac{K_1}{K_2}$	F_y	$K_{eff}@D_D$	D_D (cm)
1	2	6	0.02W	0.065W	7.2	0.0235W	0.01W	20.5
2	2	16	0.04W	0.065W	8.8	0.046W	0.01W	15.5
3	2	27	0.06W	0.065W	11.8	0.065W	0.01W	13
4	2.5	8	0.02W	0.04W	7.2	0.0235W	0.0064W	23.9
5	2.5	21	0.04W	0.04W	10	0.046W	0.0064W	17.5
6	3	11	0.02W	0.025W	6.8	0.0235W	0.0044W	26.1

3. Ground motion

In order to obtain more reliable results, 13 near field ground motions are selected from PEER strong motion database. These records were selected to cover variety of parameters such as PGA, PGV and station distance from fault and also earthquake mechanism. Properties of chosen records are presented in table 4. It is recognized that the characteristics of near-field earthquakes are different from far-field ones [15]. The severity of the earthquake is often measured by the PGA while for the near-field records this is not always true. The near-field ground motions may contain high PGA value that corresponds to a short duration pulse with negligible effect on the structure. On the other hand, a low PGA with long duration pulse may have severe effects on structure. Since the PGA is

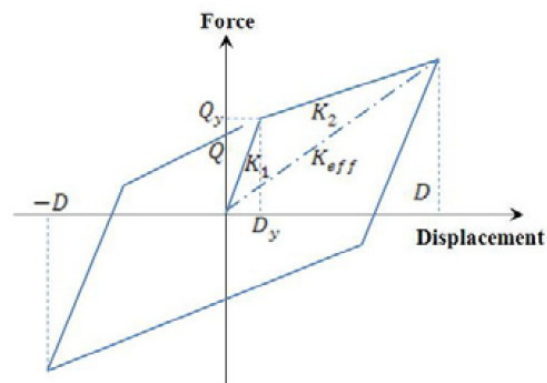


Fig. 2 Bi-linear hysteresis model of isolators

Table 4 Values of simplified formulation

Record	Station	PGA (g)	PGV (g)	Tp (Sec)
Bam	Bam	0.814	124	1.7
Cape Mendocino	89005 Cape Mendocino	1.497	127.4	0.7
Chi-Chi	TCU068	0.462	263.1	9.4
Duzce	1058 Lamont 1058	0.111	14.2	2
Erzincan	95 Erzincan	0.515	83.9	2.2
Imperial Valley	5115 El Centro Array #2	0.315	31.59	4.2
Kobe	0 KJMA	0.821	81.3	1.3
Mammoth Lakes	54099 Convict Creek	0.442	23.1	0.4
Northridge	24279 Newhall - Fire Sta	0.59	97.2	2
Northridge	77 Rinaldi Receiving Sta	0.838	166.1	1.1
Northridge	24514 Sylmar - Olive View Med FF	0.843	129.6	2.4
San Fernando	279 Pacoima Dam	1.226	112.5	1.1
Tabas	9101 Tabas	0.852	121.4	4.8

not appropriate for quantifying near-field earthquake effects, the velocity pulses (PGV) should be considered. The PGV corresponds to the integration of relatively large pulses in the acceleration time history [16]. In the near-fault region, the short travel distance of the seismic waves does not allow enough time for the high frequency content to be damped. Near-filed earthquakes may contain large amplitude long period pulses. The long period pulses in near-field records may cause strong fundamental mode shapes response of long period structures. In addition, the high frequency content of the same record may coincide with the second or higher modes resulting in severe overall response of the structure [15].

4. Modal shapes of structure and results of nonlinear dynamic analysis

By examining the modal analysis results, it is demonstrated that modal shapes of structures are very similar to each other. This similarity in modal shapes can be utilized to propose a reliable formula for base shear distribution of isolated structures.

Nonlinear time history analysis for structures consist of 2, 4 and 6 stories using 6 type of isolation systems under 13 near field earthquake records have been conducted. It is noted that in Imperial Valley, Kobe, Mammoth Lakes and Northridge-Newhall records due to content of frequencies, the effects of higher modes are more significant. In addition, for 4 and 6 story buildings or for isolation systems with high effective damping the effects of higher modes are more remarkable. The results demonstrate that static procedure for an isolated structure proposed by IBC somewhat overestimates the story force.

5. Proposed formula for base shear distribution without considering isolation system properties

Comparing mode shapes and patterns of base shear distribution shows that besides the first mode, second and third modes have effects on this distribution. Having in mind the similarities in mode shapes by simplifying first three modes (Fig.3) the following formula for base shear distribution can be derived:

$$F_x = \frac{V_s}{n+1} ([A] + \eta[B] + \rho[C]) \tag{14}$$

Where n is number of stories, $[A]$, $[B]$ and $[C]$ are vectors with $n+1$ rows according to the figure 3. The quantities of η and ρ are derived from comparison between results of

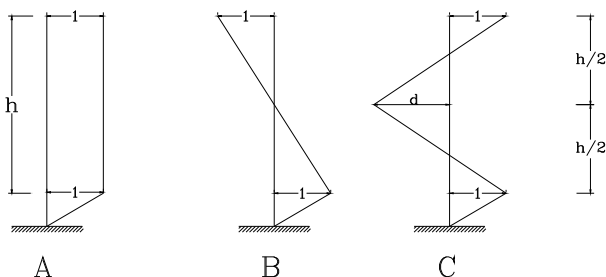


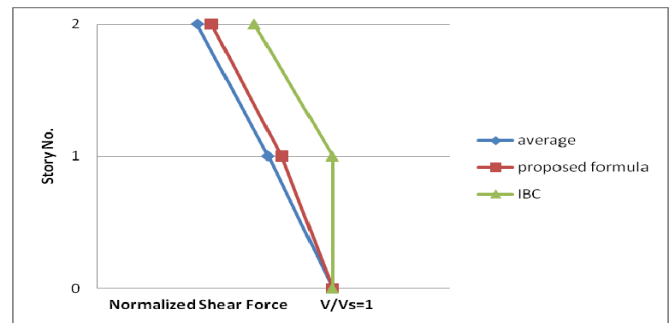
Fig. 3 Simplified mode shapes

nonlinear dynamic analysis and the previous equation as shown in table 5. Fig.4 shows comparison between shear force distributions obtained from average results of nonlinear dynamic analysis, proposed formula and IBC formula for 2, 4 and 6 story structures. It is noted that the proposed formula gives more reasonable distribution of base shear over height of structures with respect to IBC suggestion.

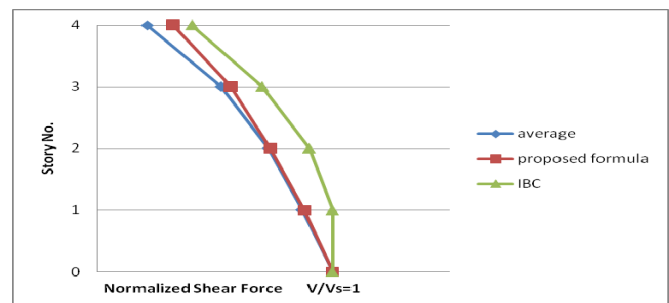
Fig.5 illustrates the bar chart of percentage error of base shear distribution obtained from nonlinear dynamic analysis results, proposed and IBC formula. It was demonstrated that the proposed formula compared to IBC formula is closer to the average results of nonlinear dynamic analysis as an exact

Table 4 Ground motions

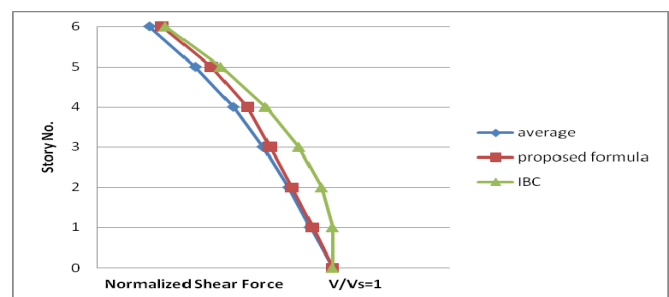
No of story	η	ρ	d
2	-0.24	0.03	2
4	-0.45	-0.06	1.5
6	-0.51	0.1	1.33



(a) 2 story building



(b) 4 story building



(c) 6 story building

Fig. 4 Comparison between distributions of shear force obtained from nonlinear dynamic analysis, proposed formula and IBC formula

Substituting equation (17) in equation (15) and multiplying by $[\chi]^T$, the nth row of obtained equation can be written as:

$$M_n \ddot{y}_n(t) + C_n \dot{y}_n(t) + M_n \omega_n^2 y_n(t) = \{\phi_n\}^T \{P_{eff}\} \quad (19)$$

$$\{P_{eff}\} = -[M][I]\ddot{x}_g \quad (20)$$

$$\{f_n(t)\} = \{\phi_n\}^T \{P_{eff}\} = -\{\phi_n\}^T [M][I]\ddot{x}_g = \bar{K}_n \ddot{x}_g \quad (21)$$

$$\bar{K}_n = \{\phi_n\}^T [M][I] \quad (22)$$

\bar{K}_n is earthquake excitation coefficient for nth mode. Equation (19) can be written as following form:

$$\ddot{y}_n(t) + 2\xi_n \omega_n \dot{y}_n + \omega_n^2 y_n = \frac{\bar{K}_n}{M_n} \ddot{x}_g(t) \quad (23)$$

Considering Duhamel's integral, $\{u(t)\}$ can be shown as follows:

$$y_n(t) = \frac{\bar{K}_n}{\omega M_n} V(t) \quad (24)$$

Where $V(t)$ is pseudo velocity.

Equation (24) can be expressed as following by substituting equation (24) into equation (17):

$$\{u(t)\} = [\chi] \left\{ \begin{array}{c} \vdots \\ \frac{\bar{K}_n}{M_n \omega_n} V_n(t) \\ \vdots \end{array} \right\} \quad (25)$$

Elastic force vector can be presented as follows:

$$\{f_s(t)\} = [K]\{u(t)\} \quad (26)$$

By substituting equation (25) into (26) elastic force vector becomes:

$$\{f_s(t)\} = [K][\chi] \left\{ \begin{array}{c} \vdots \\ \frac{\bar{K}_n}{M_n \omega_n} V_n(t) \\ \vdots \end{array} \right\} \quad (27)$$

Elastic force vector can be rearranged by using equation 22 as:

$$\{f_s(t)\} = [M][\chi] \left\{ \begin{array}{c} \vdots \\ \omega_n^2 \frac{\bar{K}_n}{M_n} V_n(t) \\ \vdots \end{array} \right\} \quad (28)$$

Since term $\omega_n^2 \frac{V_n(t)}{\omega_n}$ is acceleration type, equation (28) can be summarized for nth mode as:

$$\{f_{sn}(t)\} = [M][\phi_n] \frac{\bar{K}_n}{M_n} A_n(t) \quad (29)$$

$$M_n = \{\phi_n\}^T [M][\phi_n] \quad (30)$$

It is noted that by summation of coefficient $[M] \frac{\bar{K}_n}{M_n} A_n(t)$ in

equation (29) for all necessary modes $\{f_s(t)\}$ can be obtained. By using equation (22) and (30) the values of \bar{K}_n and M_n for each mode can be ascertained. If a relation is set for $A_s(t)$ an appropriate coefficient for each mode can be presented.

The period of isolated structure is greater than 1 second and consequently $A(t)$ can be expressed as follows according to building codes:

$$A(t) = \frac{d}{T^\lambda} \quad (31)$$

Where T is period of structure, d and λ in various codes have different values. In order to achieve a simple equation, coefficient of each mode should be divided by summation of coefficients of all modes. Herein, the discussion will be limited to the first three modes. Consequently considering appropriate value for λ parameter and using equations (32) to (34) coefficients for each mode are evaluated. Hence, the formula for base shear distribution and the relevant coefficients can be suggested as follows:

$$\alpha = \frac{\frac{\Gamma_1}{T_1^\lambda}}{\frac{\Gamma_1}{T_1^\lambda} + \frac{\Gamma_2}{T_2^\lambda} + \frac{\Gamma_3}{T_3^\lambda}} \quad (32)$$

$$\beta = \frac{\frac{\Gamma_2}{T_2^\lambda}}{\frac{\Gamma_1}{T_1^\lambda} + \frac{\Gamma_2}{T_2^\lambda} + \frac{\Gamma_3}{T_3^\lambda}} \quad (33)$$

$$\gamma = \frac{\frac{\Gamma_3}{T_3^\lambda}}{\frac{\Gamma_1}{T_1^\lambda} + \frac{\Gamma_2}{T_2^\lambda} + \frac{\Gamma_3}{T_3^\lambda}} \quad (34)$$

$$\{F\} = V(\alpha\{\phi_1\} + \beta\{\phi_2\} + \gamma\{\phi_3\}) \quad (35)$$

Where, $\Gamma_1 = \frac{\bar{K}_1}{M_1}$

Comparison of base shear distribution obtained from nonlinear dynamic analysis and the previous equations shows that for 2 and 4 story buildings parameters Γ_2/T_2^λ and Γ_3/T_3^λ , for 6 story building parameter Γ_2/T_2^λ should be negated to reach a realistic base shear distribution.

In order to simplify the equations, stiffness and mass are assumed to be equal through the stories. Comparing base shear distribution obtained from nonlinear dynamic analysis and equations (32) to (35), $\lambda=1.0$ for 2 and 4 story buildings and $\lambda=1.2$ for 6 stories building is appropriate.

Using eigenvalues problem, natural frequencies can be obtained as follow and for 2 story building:

$$Det \begin{bmatrix} k_{eff} + k & -k & 0 \\ -k & 2k & -k \\ 0 & -k & k \end{bmatrix} - \begin{bmatrix} m & 0 & 0 \\ 0 & m & 0 \\ 0 & 0 & m \end{bmatrix} \omega^2 = 0 \quad (36)$$

Solving above equation results:

$$-m^3 \omega^6 + (4knt^2 + m^2 k_{eff}) \omega^4 - 3(k^2 m + km k_{eff}) \omega^2 + k^2 k_{eff} = 0 \quad (37)$$

Assuming $\frac{k_{eff}}{k} = \theta$ and $\frac{\omega^2}{\omega_n^2} = X$ yields:

$$-X^3 + (4 + \theta)X^2 - (3 + 3\theta)X + \theta = 0 \quad (38)$$

Considering various values for θ and using the previous equation natural frequencies and modal shapes can be obtained. Utilizing equations (22) and (30) results \bar{K}_n and M_n for various θ values. Eventually by using equations (32) to (34) the coefficients α , β and γ for various θ values can be obtained. The results of this method for 2-story building are illustrated in figs. 6-8. Continuing this method for 4 and 6 story buildings provides to calculate α , β and γ coefficients.

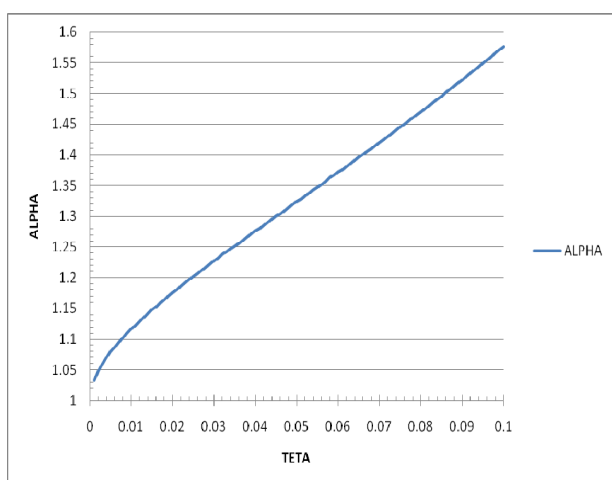


Fig. 6 Coefficient α versus various θ values for 2 story building

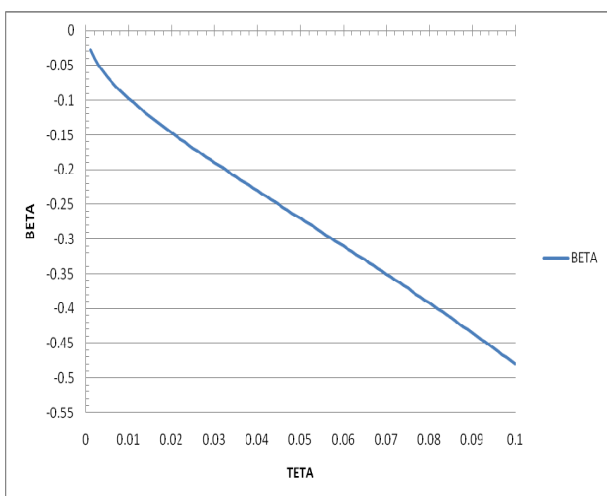


Fig. 7 Coefficient β versus various θ values for 2 story building

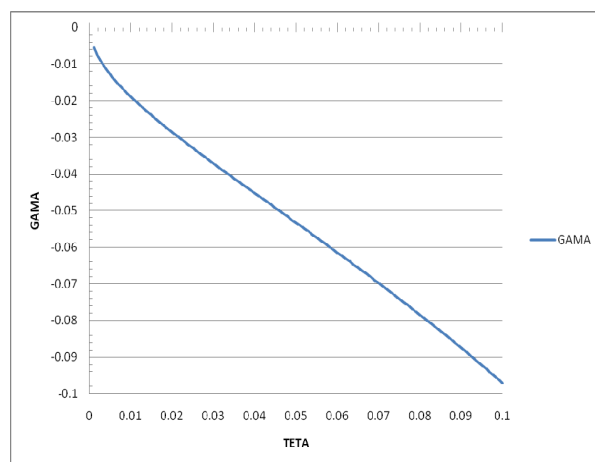


Fig. 8 Coefficient γ versus various θ values for 2 story building

6.2. Comparison of proposed formula and results of nonlinear dynamic time history analysis

In this section the results of nonlinear dynamic analysis under 13 near field earthquakes are compared with IBC and proposed formula presented in section 5 and 6 of this paper. It is noted that the results of proposed formula presented in section 6 (named proposed formula) is closer to nonlinear dynamic analysis than formula suggested in section 5 (named previous formula) (Figs.9-14).

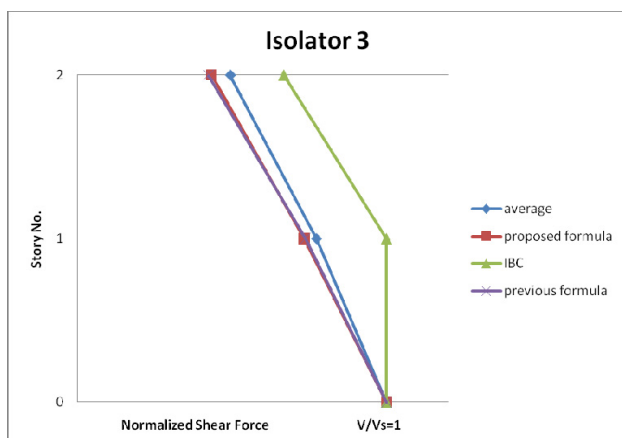
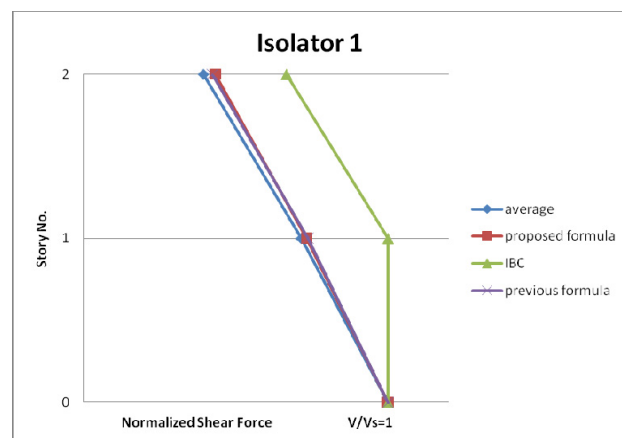


Fig. 9 Comparison of nonlinear dynamic analysis, IBC formula, proposed formula in section 6 and previous formula for 2 story building

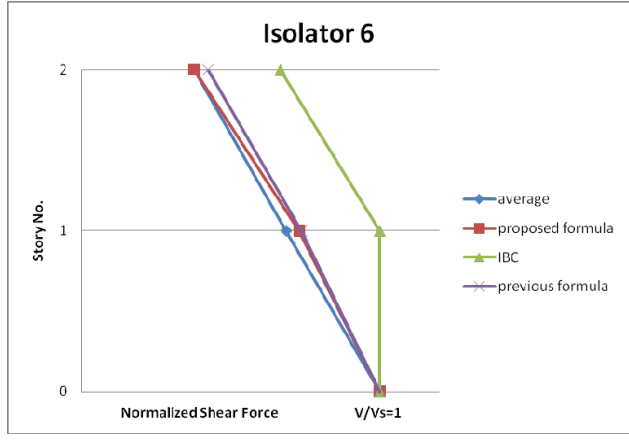
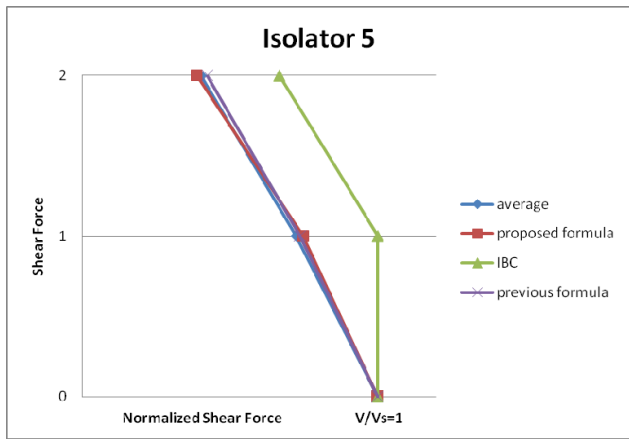


Fig. 10 Comparison of nonlinear dynamic analysis, IBC formula, proposed formula in section 6 and previous formula for 2 story building

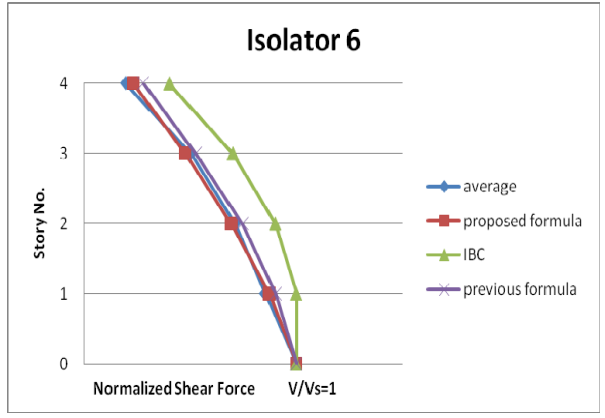
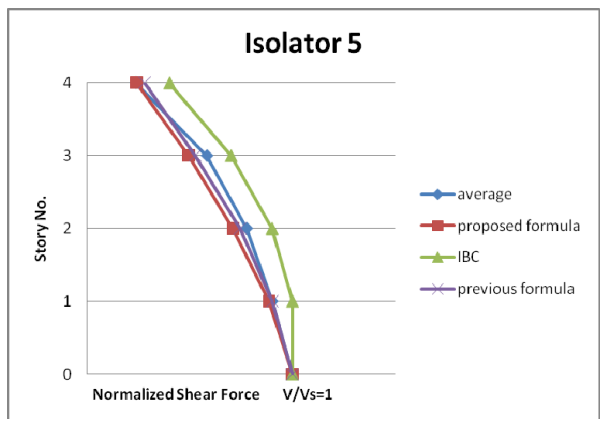


Fig. 12 Comparison of nonlinear dynamic analysis, IBC formula, proposed formula in section 6 and previous formula for 4 story building

Figs.15 shows the error of base shear distributions obtained from proposed formula in section 6 and 5. Comparing results of suggested formula in section 6 and 5 it has been noted that most of the studied cases have negligible error in comparing to the average results of nonlinear dynamic analysis.

In addition, the previous figure illustrates that for 4 and 6 story buildings the difference between two formulas are more significant than 2 story building. Otherwise, it is observed that maximum percentage error occurs in isolation system type 6

while the isolation period is 3 second. According to the models, isolation systems type 1, 2 and 3 have periods equal to 2s, periods of isolation systems type 4 and 5 are equal to 2.5s and for isolation system type 6 the period is 3s. It is noted that the average results obtained from nonlinear dynamic analysis and proposed formula in section 5 has more error using isolation system type 6. Since the properties of isolation systems have been included in the proposed formula (section 6) the errors become less. It shows the advantage of the proposed formula in section 6.

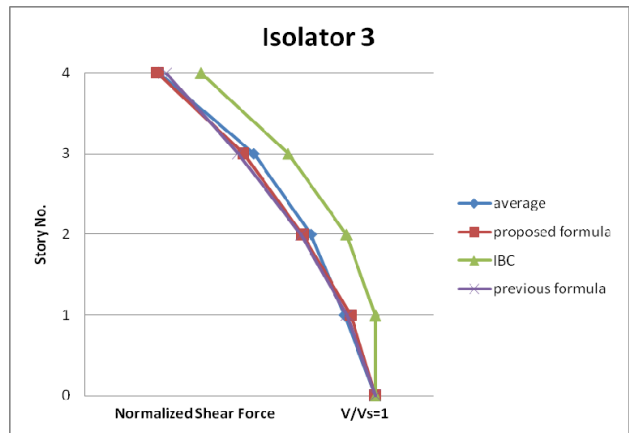
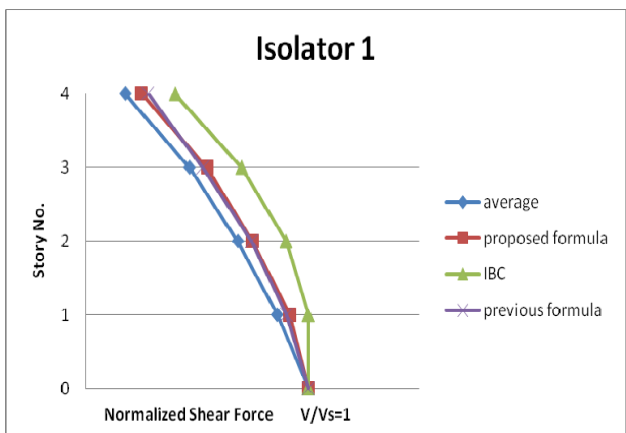


Fig. 11 Comparison of nonlinear dynamic analysis, IBC formula, proposed formula in section 6 and previous formula for 4 story building

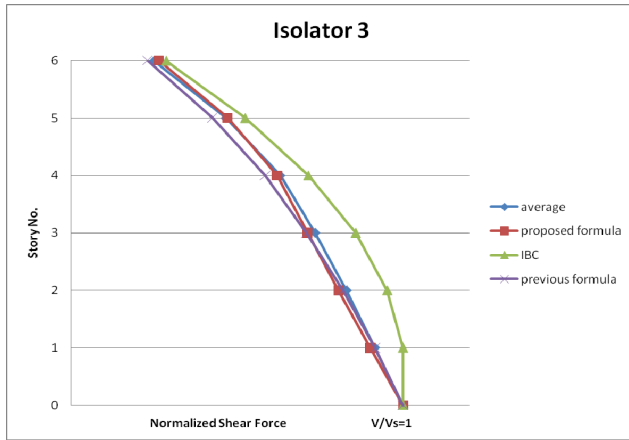
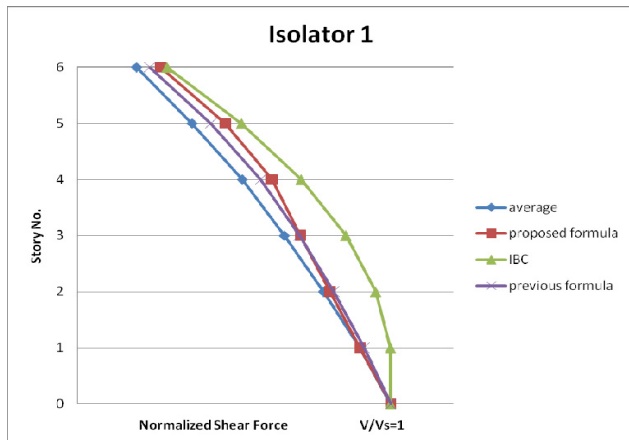


Fig. 13 Comparison of nonlinear dynamic analysis, IBC formula, proposed formula in section 6 and previous formula for 6 story building

7. Conclusion

This paper focuses on suggestion a new formula for vertical distribution of base shear over height of isolated structures. For this purpose 2, 4 and 6 story buildings assuming symmetric in plan and height were studied. For verification of proposed formulas for base shear distribution, nonlinear dynamic analysis of isolated structures under thirteen near field earthquakes were considered as an exact solution. The results obtained from nonlinear dynamic analysis, IBC and

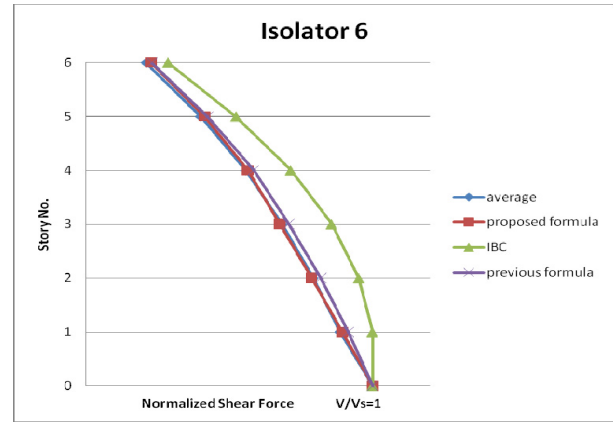
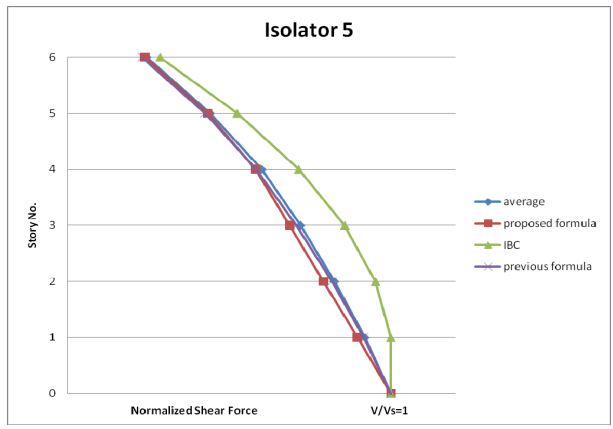
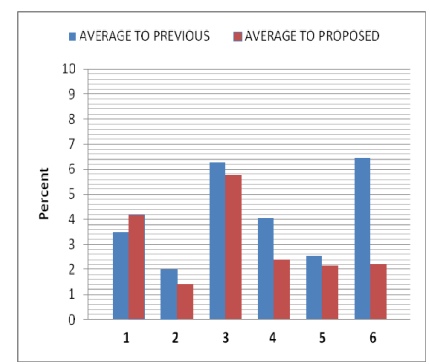
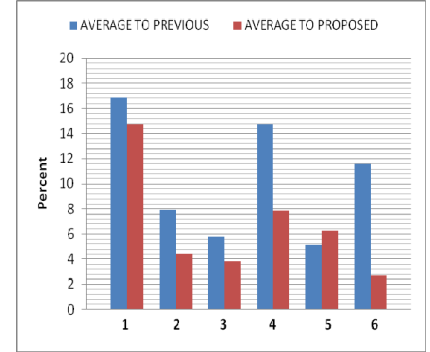


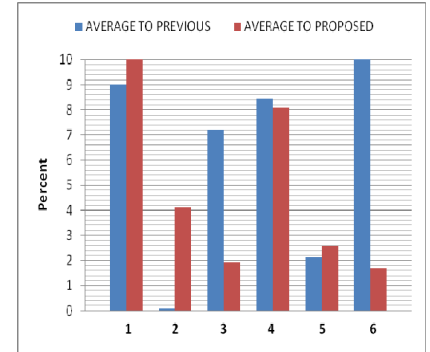
Fig. 14 Comparison of nonlinear dynamic analysis, IBC formula, proposed formula in section 6 and previous formula for 6 story building



(a) 2 story building



(b) 4 story building



(c) 6 story building

Fig. 15 Comparison of previous and proposed formula to nonlinear dynamic analysis for various isolation systems

two proposed formula lead to the following results:

1. Base shear distribution of isolated structures falls between uniform and triangular distribution. The suggested formula in IBC overestimates shear story which consequently omits the capability of the isolation system in reducing forces transmits to superstructure.

2. Considering the nonlinear behavior of isolation systems, due to change in stiffness of isolation systems, wide range of periods is transmitted from isolation system to superstructure. As a result higher modes contribute in response of structure. Hence, the effects of higher modes should be considered in response of structure.

3. Proposed formula presented in section 5 is almost near to average results obtained from nonlinear dynamic analysis, however, this formula is independent in properties of isolation system, and i.e. for a building with variety of isolation systems this formula is identical.

4. Another formula was proposed in section 6 and it is function of effective stiffness and period of isolation system. Thus by changing the properties of isolation system the coefficients of first three modes change too. Consequently pattern of base shear distribution will change too.

5. According to the comparison of proposed formulas and nonlinear time history analysis as an exact solution, the accuracy of formulas was demonstrated by illustrating the errors of various cases. In addition, these results confirm the contribution of higher modes on vertical distribution of base shear over height of isolated structures.

References

- [1] Yang, Y.B, Chang, K.C, and Yao, J.D, " Base Isolation", Earthquake Engineering Handbook,2003.
- [2] Naem, F., Mayes., R.L., "Design of structures with seismic isolation", Seismic Design Handbook, CA, USA, 2001.
- [3] Wang, Yen-Po., "Fundamentanls of Seismic Base Isolation", International Training Programs for Seismic Design of Building Structures.
- [4] Uniform Building Code "UBC-91", International Conference of Building Officials, Chapter 23, Whittier, C.A, USA, 1991.
- [5] Uniform Building Code "UBC-97", International Conference of Building Officials, Chapter 23, Whittier, C.A, USA, 1997.
- [6] International Buliding Code, 2010.
- [7] European Committee for Standardization (CEN), Eurocode 8: Design of Structures for Earthquake Resistance, 2010.
- [8] New Zealand Standard, Structural Design Actions, 2010.
- [9] Lee, D.G, Hong, J.M., and Kim, J., "Vertical distribution of equivalent static loads for base-isolated building structures", Journal of Engineering Structures, 2001, pp1293-1306.
- [10] Cardone, D., Dolce, M., and Gesualdi, G., "Lateral force distribution for the linear static analysis of base-isolated buildings", Bull Earthquake Eng, 2009, pp801-834.
- [11] Khoshnoudian, F., Esrafil, S., "A new lateral force distribution formula for base-isolated structures", Institution of Civil Engineering Journals, 2008, pp277-297.
- [12] Khoshnoudian, F., Mehrparvar B., "Evaluation of IBC equivalent lateral response procedure for base shear distribution of seismic isolated-structures", Journal of Earthquake Engineering, Vol12, 2008, pp681-703.
- [13] American Institute of Steel Construction (AISC).
- [14] Park, Y.J., Wen, Y.K. and Ang, A.H., "Random vibration of hysteretic systems under bi-directional ground motions", Earthquake Engineering and Structural Dynamics, Vol 14, 1986, pp.34-53.

- [15] Ghobarah, A., "Response of structure to near-fault ground motion", World Conference on Earthquake Engineering, Vancouver, Canada, 2004.
- [16] Elsheikh, A., Ghobarah, A., " Response of RC structures to near-fault records", Emirates journal for Engineering research, 2004, pp45-51.
- [17] PEER (Pacific Earthquake Engineering Research Center) Strong Motion Database, University of California, Berkeley, <http://peer.berkeley.edu/>.
- [18] Nagarajaiha, S., Reinhorn, A.M. & Constantinou, M.C. (1993). 3D-BASIS : Computer program for nonlinear dynamic analysis of three dimensional base isolated structures. NCEER-93-0011, National Center for Earthquake Engineering Research, Buffalo, N.Y.
- [19] Wen, Y.K. (1979). Method of random vibration of hysteretic systems. Journal of Engineering Mechanics, ASCE, No. 102, 249-263.

Notation

V_s	calculated base shear from code formula
w_x, w_i	weight of stories at x and i levels
h_x, h_i	height of stories at x and i levels
F_x, m_x	force and mass at x level
T_{eff}, S_{eff}	effective period and effective damping of isolation system
S_e	spectral acceleration
C_{vx}	vertical distribution coefficient
ε	square ratio of isolation system frequency to superstructure frequency
μ	effective height coefficient
h_n	height of the structure
$\Delta_{1i}, \Delta_{2i}, \Delta_{3i}$	profile of displacement
$\phi_{1i}, \phi_{2i}, \phi_{3i}$	first three mode shapes
a_2, a_3	coefficients related to characteristics of isolation system and superstructure
$[A],[B],[C]$	first three simplified mode shapes of isolated structures
η, ρ	factors related to second and third mode shapes contribution
n	number of stories
K_1, K_2, K_{eff}	initial, secondary and effective stiffness respectively
Q	intersection of hysteresis cycle and vertical axis
T	period of super-structure
D_y	yield displacement
$[M],[C],[K]$	mass, damping and stiffness matrix respectively
$\{\ddot{u}\}, \{\dot{u}\}, \{u\}$	acceleration, velocity, and displacement of structure respectively
\ddot{x}_g	ground acceleration
$\{y(t)\}$	modal coordinate
$[\chi]$	modal matrix
K_n	modal excitation factor for nth mode
M_n, C_n, K_n	modal mass, damping, and stiffness for nth mode
ξ_n	damping ratio for nth mode
$\dot{V}(t)$	pseudo velocity
$\{f_s(t)\}$	elastic force vector
Γ_1	participation factor of first mode
α, β, γ	factors corresponding to first, second and third mode shapes contribution
θ	ratio of K_{eff} to stiffness of story